Models for quasicrystal–crystal epitaxy

E J Widjaja and L D Marks

Department of Materials Science and Engineering, Northwestern University, Cook Hall,
2220 Campus Drive, Evanston, IL 60201-3108, USA

Abstract
Not long after the discovery of quasicrystals, a specific orientation relationship between
crystalline and quasicrystalline structures was observed. The specific orientational relationships
were discovered in many systems, for instance surface alterations of bulk quasicrystals, the
growth of atomic overlayers on quasicrystalline substrates and quasicrystalline thin films on
crystalline substrates. In this paper, we review various models described in the literature in
explaining such quasicrystal–crystal epitaxy.

(Some figures in this article are in colour only in the electronic version)

1. Introduction

Since the discovery of quasicrystals [1], a fair amount of research has looked to understand the relationship between the quasicrystalline and crystalline structures. One particular area has been the interface between the two structures. Shortly after its discovery, it was established that bombardment of icosahedral Al–Mn by Ar ions at room temperature transforms the quasicrystalline surface into a crystalline cubic structure due to preferential sputtering of aluminum from the surface [2]. The resultant crystalline structure has a specific orientation relationship with respect to the quasicrystalline substrate.
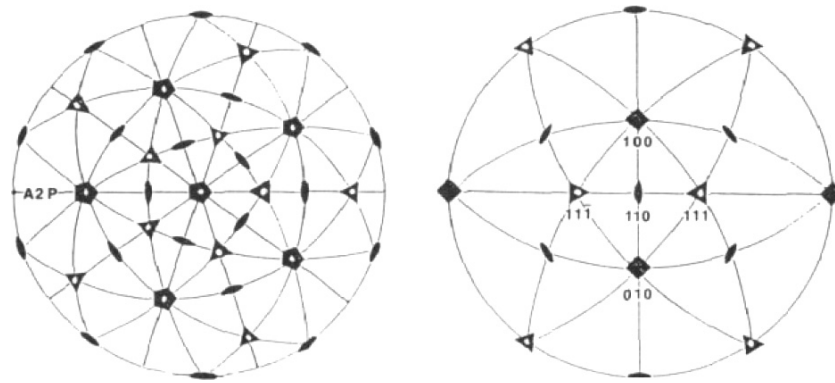
This specific orientation relationship between the crystalline–quasicrystalline phases in Al–Mn alloys has triggered research into other quasicrystalline structures. Similar observations were soon observed in systems such as decagonal $Al_{70}Ni_{15}Co_{15}$ [3, 4], icosahedral $Al_{65}Cu_{20}Fe_{15}$ [5, 6], decagonal $Al_{70}Cu_{15}Co_{15}$ [7, 8] and decagonal $Al_{75}Ni_{10}Fe_{15}$ [9].

In attempts to produce quasicrystalline structures in simpler material systems, thin layers of various metals were deposited in vacuum on top of quasicrystalline substrates. Shimoda *et al* investigated the growth of Au [10, 11] and Pt [12] on decagonal Al–Ni–Co surfaces. By using indium as a surfactant to promote two-dimensional growth and annealing at temperatures about 500 K, they observed the formation of ten different domains of $AuAl_2$ and $PtAl_2$ alloys with (110)-type surface plane with alignment of the symmetry axes. In further work, elements such as Ag, Al, As, Au, Bi, Co, Cu, Fe, Na, K, S, Si and Pt have been deposited on various surfaces of quasicrystalline substrates, such as Al–Pd–Mn, Al–Cu–Fe and Al–Ni–Co. A rather exhaustive list is provided in a recent review by Sharma *et al* [13]. Recently, Longchamp *et al* [14] reported a well-ordered ultrathin aluminum oxide on

icosahedral AlPdMn quasicrystal with (111) faces parallel to the fivefold symmetry surface. A recent review by Fournée and Thiel [15] gives an overview of solid films on quasicrystalline substrates.

The third method for creating crystalline–quasicrystalline interfaces with specific orientation relationships is the inverse of the former, i.e. thin layers of quasicrystalline films are deposited on crystalline substrates. Li *et al* first reported growth of fully oriented Al–Cu–Co decagonal films on crystalline substrates but were unable to study the geometric orientations at the interface [16]. Widjaja and Marks presented evidence of epitaxial Al–Cu–Fe–Cr decagonal thin films on atomically flat $Al_2O_3(0001)$ surface [17]. Brien *et al* [18] reported growth of textured icosahedral Ti–Ni–Zr thin films on $Al_2O_3(0001)$ by pulsed laser deposition with one of their fivefold symmetry axes slightly tilted ($\sim6°$) to the substrate surface. Later, Willmott *et al* [19] grew similar film showing the fivefold symmetry axes to be perpendicular to the substrate surface. These films however have random orientation of the twofold axes in-plane. Saito *et al* [20] reported growth of a decagonal phase in an Al–Ni–Co film deposited on (0001) sapphire substrate with twofold axes oriented to the substrate surface. Saito *et al* observed, like Widjaja and Marks [17], that there are two preferred in-plane orientations, with the tenfold symmetry aligned to $\langle 3\bar{3}00 \rangle$ and to $\langle 11\bar{2}0 \rangle$ of the substrate.

By creating quasicrystalline thin films on crystalline substrates, one has further freedom for specific applications. Recently, Franke *et al* [21] suggested the potential of quasicrystalline interlayers to epitaxially link incommensurate materials. However, this work has to date been limited by the difficulty of controlling the quality of the quasicrystalline films via vacuum deposition, specifically the controlling of composition [22, 23].

0953-8984/08/314003+08$30.00

1

Figure 1. Stereographic projection diagram showing the orientational relationship between the (a) quasicrystal and (b) B2-type phase. Reprinted from [24], copyright (1993) by the Institute of Physics.

This purpose of this paper is review the various quasicrystalline–crystalline epitaxy models which have been proposed to explain the orientational relationships.

2. Models for quasicrystal–crystal epitaxy

As described above, there is now a fair amount of experimental data for orientational/epitaxial relationships between quasicrystalline materials and conventional crystalline materials, as well as some data for quasicrystal–quasicrystal systems. (For reference, since there is sometimes some disagreement in terms of definitions of epitaxy, we will define it here as the case when there is a well-defined orientational relationship between the two phases, which therefore includes cases such as cube-on-cube epitaxy as well as van der Waals epitaxy.) This necessarily means that this is at least a local minimum of the interfacial free energy between the two phases. Unfortunately, because it is often hard to describe a quasicrystalline material in a way that allows one to calculate this interfacial energy, in some cases the models have been only qualitative or semi-qualitative, or borrow from models for conventional crystal–crystal interfaces. We will detail below the main analyses to date.

2.1. Stereographic projection through a description of the rotation axis alignment

The majority of work employing ion bombardment of quasicrystalline surfaces resulting in an overlayer of crystalline structures has explained the observed orientation from a stereographic projection through a description of the rotation axis alignment. Such descriptions were made for various quasicrystal structures such as icosahedral Al–Cu–Fe [5, 24, 25] and decagonal Al–Ni–Co [4]. The description of the rotation axis alignment typically states a pair of axes, one belonging to the quasicrystalline and the other to the crystalline structures. Typically, two types of alignment are mentioned, the out-of-plane and in-plane alignments.

In their experiments, Wang *et al* [24] irradiated an $Al_{62}Cu_{25.5}Fe_{12.5}$ icosahedral quasicrystal at room temperature with 120 keV Ar^+ ions to induce transformation to the B2-type crystalline phase. Electron diffraction patterns reveal

the orientation relationship as: A5(QC) ∥ [110](B2), A2(QC) ∥ [11$\bar{1}$](B2), where A5(QC) and A2(QC) represent the fivefold and twofold axes of the quasicrystals, respectively. The relationship was further illustrated by means of two stereographic projection diagrams for the quasicrystal (figure 1(a)) and B2 phase (figure 1(b)) which are parallel to each other. A similar approach was taken by Shen *et al* [26], as shown in figure 2, with additional starting points as described in section 2.2.
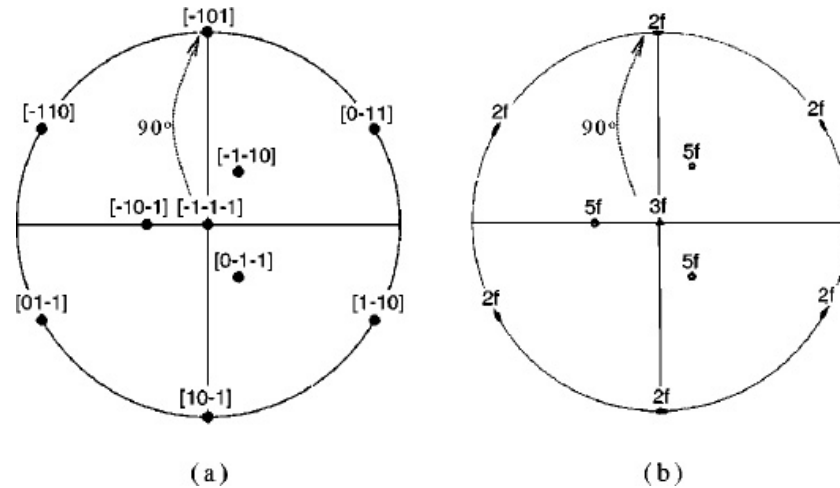
In their paper, Shalaeva and Prekul [25] took the approach of Wang *et al* one step further by calculating the angle of azimuthal misorientation between rows of reflections of the quasicrystalline–crystalline diffraction patterns taken along a specific direction.

While the method of stereographic projection through a description of the rotation axis alignment is a valid approach for describing the orientation, this method offers no insight into the fundamental mechanism behind the preferred orientation.
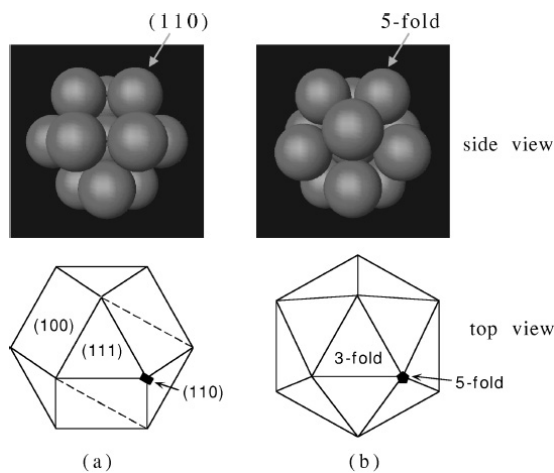
2.2. Close relationship of structural model

One of the methods used to analyze high angle grain boundaries in conventional crystals is the structural unit model (e.g. [27–29]). The idea is that these boundaries have a low free energy if they are composed of structural units which match both sides of the boundary and are repeated along the boundary. One can extend this idea to quasicrystals by looking for cases where the crystal and quasicrystal have similar structural elements which can therefore form low energy interfacial units.

As an example of this approach, Shen *et al* [26] explained the orientation relationship between different surfaces of icosahedral Al–Cu–Fe and its cubic phase via a structural model of cubic close packed and icosahedral packed clusters. They started with a simple structural model: packing of equal spheres. In both cubic close packing (ccp) and icosahedral packing (ip) of equal spheres, each sphere is surrounded by 12 nearest neighbors. In icosahedral packing the middle layer is buckled instead of planar and rotated by 30°, compared to ccp. On the basis of this transformation, it was concluded that there is a close relationship between the symmetry axes of these two types of packing. This relationship was further shown in stereographic projections. Figure 3 compares the ccp (111) and the ip threefold projections.

Figure 2. Stereographic projection of (a) cubic [111] zone axis; (b) icosahedral threefold zone axis. The high symmetry axes that are parallel, or nearly so, in the two structures are labeled. Reprinted from [26], copyright (1998) by the American Physical Society.

Figure 3. Structure models of (a) cubic close packed (ccp) cluster; (b) icosahedral packed (ip) cluster. Top row: side view; bottom row: top view. The three [110]-type axes of ccp that are perpendicular to the [111] axis are lined up with the three twofold axes of ip. The other three (110)-type axes of ccp that are 35.26° away from the (111) axis are almost parallel to three fivefold axes of ip (2.1° off). Reprinted from [26], copyright (1998) by the American Physical Society.
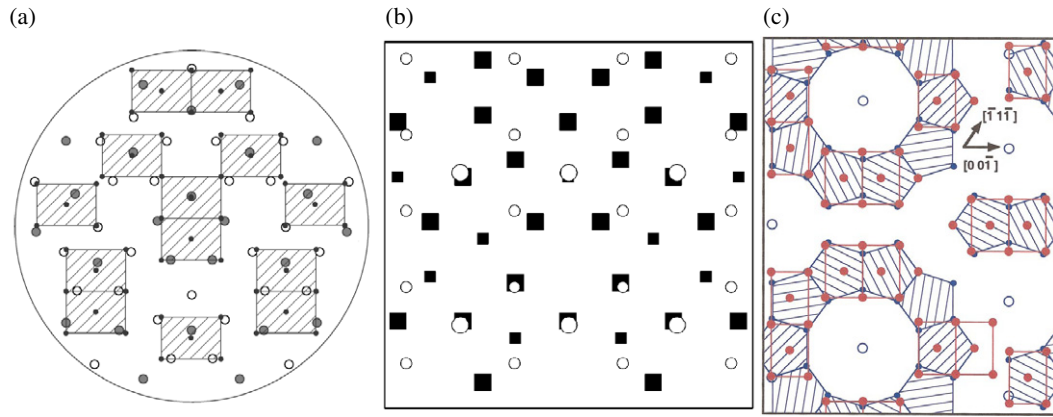
2.3. Atomic model of the two-dimensional interface between the quasicrystal and crystal phases (coincidence site lattice)

One approach to the epitaxial growth places importance upon the principle that the coherent overgrowth of crystal material Y on crystal X is likely to occur if some undistorted crystal plane of Y can be laid down on top of the exposed face of X, in such a way that a large fraction of the Y atoms can be made to coincide with the sites of X atoms. It can be further understood that the greater the number of coincidences per unit area, the lower the energy of the resulting interface will be. This basic principle is the backbone of the coincidence site lattice (CSL) theory which was first investigated by Friedel [30], and later explored by Ranganathan [31], and applied to cubic lattices by Grimmer [32–35].

This method has been adopted by Shimoda *et al* [10], Zurkirch *et al* [3], and Bolliger *et al* [36] as summarized in table 1, who described their findings via an atomic model of the two-dimensional interface between the quasicrystal and crystal phases, which is obtained by superimposing the surface structures. Their models implicitly incorporated the CSL concept; however their approach lacks the theoretical mathematical expressions that include interfacial energy. An attempt to calculate the interfacial energy using the CSL concept was carried out by Flückiger *et al* [37].

Zurkirch *et al* [3] presented the orientational relationship between two phases, decagonal Al–Co–Ni and its bcc phase upon sputtering, and a structural model for the epitaxial growth at the interface. They showed that a [110] axis of the bcc phase is oriented parallel to the tenfold symmetry direction, while for the twofold axes: $A_{2P} \parallel \langle 110 \rangle$ and $A_{2D} \parallel \langle 111 \rangle$ and $\langle 110 \rangle$. The model conjectures that the interface between the bulk quasicrystal and the cubic units at the surface is atomically abrupt. A few (110) planes of the bcc structural unit were superimposed onto an atomic model suggested for AlCoNi [38], with the orientation chosen according to the experimental result, as shown in figure 4(a). They claim a satisfactory agreement between the cubic phase and most of the Al and transition-metal atoms. The small mismatch between the two phases was considered as caused by the lack of a long-range ordered crystalline surface layer.

Similarly, Shimoda *et al* [10] describe their finding in an attempt to grow epitaxial quasicrystalline films of Au on the tenfold surface of Al–Ni–Co. Upon annealing, an epitaxial AuAl$_2$ layer was formed with the (110) surface oriented to the tenfold surface. RHEED patterns were interpreted as alignment of the A2D axis with [001] and [$\bar{1}$12] and of the A2P axis with [$\bar{1}$11] and [$\bar{1}$10] incidences. The lattice constant was estimated at 0.6 nm, close to 0.5998 nm for the CaF$_2$-type AuAl$_2$. A model was built, as shown in figure 4(b), showing the mismatch between the pentagonal units in the quasicrystal phase and the crystalline lattice of the AuAl$_2$ phase to be locally small.

Figure 4. Atomic models for various interfaces showing the coincidence site lattice model by superimposing the quasicrystalline and crystalline surface atoms. (a) The interface between the (110) surface of a bcc structure and the surface of the decagonal Al–Co–Ni. Filled circles denote transition-metal and empty circles Al atoms, while small circles represent the atoms on the (110) surface of the bcc lattice. The atomic distance for the crystalline surface is 0.28 nm, as given in the crystal data for AlCo or AlNi. Reprinted from [3], copyright (1998) by the American Physical Society; (b) the interface between the AuAl$_2$ overlayer and the Al–Ni–Co substrate. Large and small circles represent Au and Al in the overlayer, respectively. Large and small solid squares represent Al and transition metals in the quasiperiodic plane of Al–Ni–Co. Reprinted from [10], copyright (2000) by the American Physical Society; (c) the interface between the pentagonal surface of the icosahedral quasicrystal Al$_{70}$Pd$_{20}$Mn$_{10}$ (smaller grey (blue online) filled circles and hatched pentagons) and the (110) surface of bcc structural units (larger grey (red online) filled circles). Reprinted from [36], copyright (1998) by the American Physical Society.

Table 1. Various epitaxial crystal structures on quasicrystalline substrates and their corresponding atomic distances showing coincidence site lattice models.

Quasicrystalline substrate		Crystalline layer			
Structure	Atomic distances	Structure	Atomic distances	Comment	Reference
Decagonal Al$_{70}$Co$_{15}$Ni$_{15}$	Citing Burkov [38]	bcc phase	0.28 nm (for AlCo or AlNi)	Show local coincidence ($\sim$2 units)	Zurkich *et al* [3]
Decagonal Al$_{72}$Ni$_{12}$Co$_{16}$	Citing Abe *et al* [39]	CaF$_2$-type AuAl$_2$	0.6 nm		Shimoda *et al* [10]
Icosahedral Al$_{70}$Pd$_{20}$Mn$_{10}$	Interatomic distance: 2.964 Å. Pentagon height: 4.561 Å	bcc phase (β-phase)	Interatomic distance: 3.05 Å along [00$\bar{1}$] compared to 1.5×3.05 Å $= 4.575$ Å	Show local coincidence ($\sim$2 units). Along [00$\bar{1}$], mismatch of 0.3%	Bolliger *et al* [36]

A study of the icosahedral Al$_{70}$Pd$_{20}$Mn$_{10}$ system by Bolliger *et al* [36] shows the orientational relationship between the icosahedral structure and its corresponding bcc phase (β-phase) upon ion bombardment. The coincidence site lattice was shown to have a small mismatch between the β and the quasicrystalline lattice, of 0.3%. Along the [00$\bar{1}$] direction the height of the pentagons is 4.561 Å, comparable to the length of the 1.5 lattice constant of the B2 structure along this direction, as shown in figure 4(c).
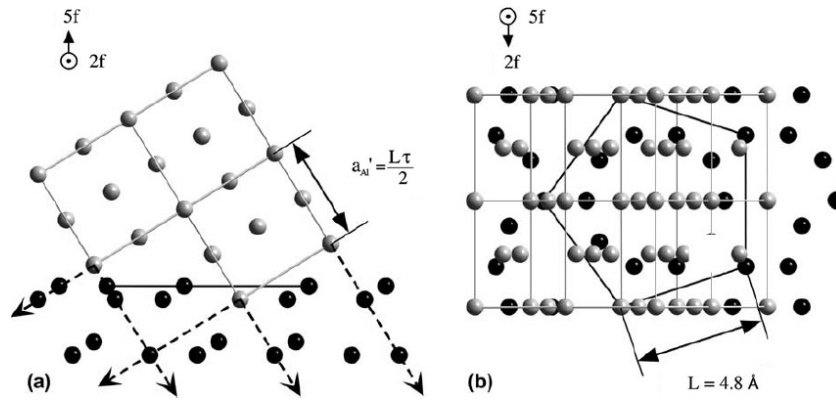
Because of the two-dimensional character of the problem, an atomistic approach is required to relate the complicated quasicrystalline structure to its crystalline counterpart. The validity of these atomic models relies heavily on a real-space structural model for the quasicrystal system, which may not be readily available or, in some cases, may not be correct. Furthermore, their models fall short of the long-range fitting for the superimposed structure since misfit dislocations and interface relaxations are ignored.

In another paper, Bolliger *et al* [40] reported growth of Al nanocrystals on icosahedral Al–Pd–Mn substrate, with their [111] axes aligned parallel to threefold axes of the substrate at
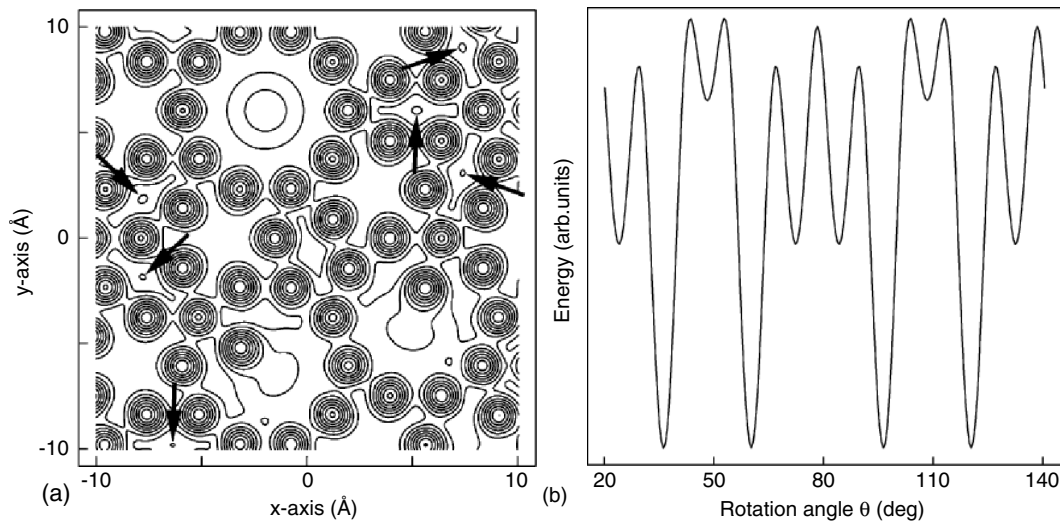
37.37° away from the surface normal. This growth mode has no high symmetry facets of the crystalline structure parallel to the substrate surface. In a related paper, Lüscher *et al* [41] describe this interface configuration using coincidence site lattice. Further, they remark upon the similarity of the packing density between the fcc [100] axis and the quasicrystal substrate, along the fcc $\langle 100 \rangle$ direction. The interface configuration for Al nanocrystallite and the quasicrystal substrate described as a coincidence lattice model is shown in figure 5.

An attempt to explain the orientational relationship through energy calculations, in real space, was carried out later by Flückiger *et al* [42], using a rigid-lattice atomic model for the interface between a cubic and the decagonal surface. The calculation was carried out to explain the observed size, distribution and orientation alignment of Al islands on decagonal Al–Co–Ni. A Lennard-Jones potential was used to model the interaction between Al adsorbate atoms and the quasicrystal substrate, consisting of a surface and a subsurface layer, for a diameter of 50 Å for the substrate and up to 36 Å for the adsorbate cluster. The quasicrystalline substrate was considered to act only as a structural template and the

Figure 5. Interface configuration for Al nanocrystallite on the fivefold surface of Al–Pd–Mn. The quasicrystal surface (black atoms) corresponds to a section of the $z = -4.08$ Å termination of the bulk model. The Al lattice is represented by gray atoms with $a_{Al} = 4.05$ Å. (a) Side view along a twofold direction of the substrate which coincides with the [100] axis of the fcc lattice. (b) Top view. The fivefold direction is parallel to the $(0, 1, \tau)$ direction in the Al crystallite. The dotted arrows illustrate atomic rows along $\langle 100 \rangle$ axes of the Al nanocrystal that coincide with corresponding rows along twofold directions of the icosahedral substrate. Reprinted from [41], copyright (2004) by Elsevier.

Figure 6. (a) Constant-energy contour plots in the x–y plane. Arrows point to equivalent locations of absolute energy minima. (b) The energy as a function of the adsorbate rotation angle θ in a range of $20°$–$140°$. The adsorbate structure has a diameter of 24 Å, and the center of rotation is set at one of the absolute energy minima plotted in (a). $\theta = 0°$ is an orientation of the Al (111) plane with respect to the substrate in agreement with experimental results. Reprinted from [42], copyright (2003) by the American Chemical Society.

interaction between an adsorbate and an individual substrate atom was assumed to be averaged out.
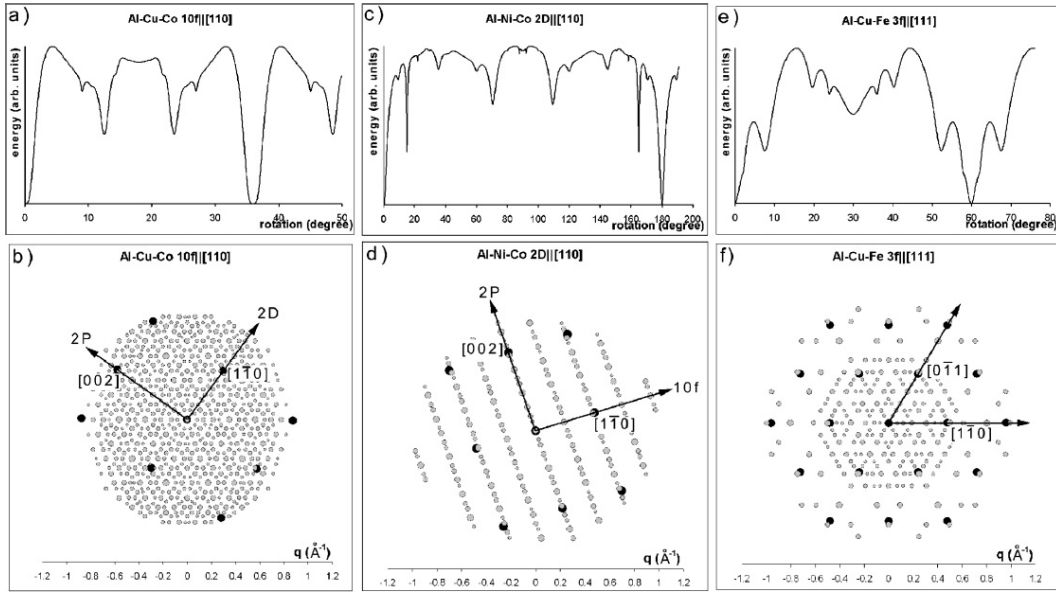
Their energy calculations were divided into two steps. The first step is to identify the location of the seed Al atom, by modeling the absolute minima of an Al atom over the substrate, using the coordinates of the quasicrystalline surface atoms (figure 6(a)). It is assumed that these locations will act as a seed for the growth of Al clusters. In the next step, the calculation was carried out for the rotational alignment of the fcc (111) layer with respect to the quasicrystal surface. The result of the energy calculation is shown in figure 6(b), showing agreement with the experimental results.

2.4. Coincidence reciprocal lattice planes

One problem with the earlier approaches is that they are either qualitative, or one has to make approximations when calculating the energy, for instance using clusters or approximants for the quasicrystals. This is because most energy calculations require that the problem be analyzed in real space.

An alternative approach was developed by Widjaja and Marks [17, 43], who based their work on a coincidence reciprocal lattice plane (CRLP) model, one previously developed by Fletcher [44] for crystal–crystal epitaxy. This model expands the energy of the interface as a combination of a long-range elastic strain field and a local pairwise potential term. Rather than numerically solving the problem, a first-order analytical model was developed by Fletcher which can be directly evaluated in most cases. What the model predicts is that when there is near coincidence of reciprocal lattice vectors the interfacial energy is small. In many respects this is equivalent to a conventional periodic CSL model (or near CSL model), but rather than evaluation in real space everything

Figure 7. Interfacial energy calculation and its corresponding structure, respectively, at 0° rotation (which is the minimum) for (a) and (b) Al–Cu–Co 10f ∥ [110], (c) and (d) Al–Ni–Co 2D ∥ [110], and (e) and (f) Al–Cu–Fe 3f ∥ [111]; crystal–quasicrystal epitaxy is due to ion bombardments. Gray and black spots represent the quasicrystal and crystal spots, respectively. Reprinted from [43], copyright (2003) by the American Physical Society.

is done in reciprocal space. This circumvents the problem of describing a real-space structure, and only needs the well-defined reciprocal space of the complex real-space quasicrystal structure which can be directly deduced from the electron diffraction patterns.

The original CRLP model of Fletcher and Lodge [45] was exploited as the starting point, with an extension (correction) of the original derivation which employs a simple basis for the unit cell with a term to more fully include the crystallography which, by analogy to crystallographic direct methods, is referred to as a unitary structure factor [46]. The CRLP model results in an equation:

$$E \sim E_0 - t \sum_k ([U(q)v(q)]^2/\kappa)$$

where E is the total interfacial energy, E_0 is the coincidence part of the boundary energy, t is a constant, κ is the vector joining two diffraction spots from the bicrystal, $U(q)$ is a unitary structure factor and $v(q)$ is the atomic interaction potential. The constant t, which depends on many parameters such as shear modulus, bulk modulus, and Poisson's ratio, is necessary for calculating an expected value for the total energy; however the value of this constant is not important in the calculations since only the relative magnitudes are considered.

A simpler and more primitive equation from the CRLP model was first applied to the epitaxial decagonal Al–Cu–Fe–Cr quasicrystalline thin films on flat Al$_2$O$_3$ sapphire (0001) substrates [17]. The decagonal phases in the thin films have the tenfold axis oriented parallel to the substrate surface normal, A$_{10}$ ∥ Al$_2$O$_3$[0001]. Only two unique relative orientations were observed: A$_{2D}$ ∥ Al$_2$O$_3$[10$\bar{1}$0] and A$_{2P}$ ∥ Al$_2$O$_3$[10$\bar{1}$0], where A$_{2D}$ and A$_{2P}$ represent the two types of twofold axis in the decagonal phase. The simpler CRLP model matches the
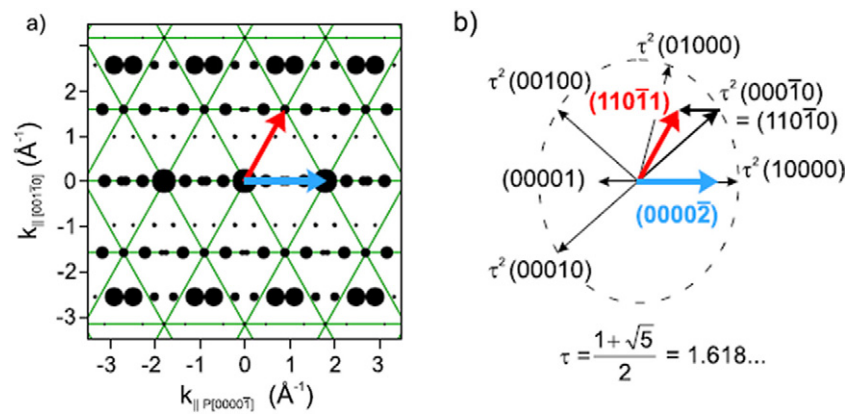
experimental observation by predicting the two unique relative orientations. The two unique orientational relationships were attributed to the coincidence reciprocal planes of (10$\bar{1}$0) of Al$_2$O$_3$ and (11100) of the decagonal, with reciprocal spacings of 2.4243 and 2.5399 nm^{-1}, and coincidence reciprocal planes of (1$\bar{2}$10) of Al$_2$O$_3$ and (12210) of the decagonal, with reciprocal spacings of 4.1990 and 4.1068 nm^{-1}.

The latter paper [43], based on above equation, carried out computations on various ion-bombarded surfaces for three quasicrystal systems: the icosahedral Al–Cu–Fe [5, 47] system and the decagonal Al–Ni–Co [3, 4] and Al–Cu–Co systems [8]. Calculations were also performed for quasicrystal–crystal thin-film epitaxy for the following systems: AuAl$_2$ [10, 11] and PtAl$_2$ [12] thin films on a tenfold surface of decagonal Al–Ni–Co and decagonal Al–Cu–Fe–Cr thin film on corundum Al$_2$O$_3$[0001] [17].

This simple model is able to explain and predict most of the experimentally observed relative orientations for epitaxy as reported in the literature. Some difficulties in fitting the simulated and observed configurations may arise from the kinetics of the system, resulting in a metastable configuration. Nevertheless, all experimental configurations appear as local minima in the energy calculations. An example of the interfacial energy calculation and its corresponding structure for Al–Cu–Co, Al–Ni–Co and Al–Cu–Fe is shown in figure 7.

In a recent paper, Franke *et al* [21] showed a similar analysis on the epitaxial growth of AlAs islands on decagonal AlNiCo. The epitaxial match at the interface was demonstrated by comparing the reciprocal lattice of the strained AlAs(111) film and the projection of the Al–Ni–Co reciprocal lattice plane, as shown in figure 8.

In a recent review by Fournée and Thiel [15], they restate that the orientational relationship between adjoining crystals is

Figure 8. (a) Reciprocal lattice match with circles depicting the reciprocal lattice of Al–Ni–Co projected onto the $(10\bar{2}\bar{2}4)$ interface plane and the vertices of the mesh of the AlAs(111) film. The radii of the circles are proportional to the Fourier amplitudes of the atomic density of Al–Ni–Co calculated from the structural model by Yamamoto and Weber. (b) Projected Al–Ni–Co reciprocal lattice vectors. Reprinted from [21], copyright (2007) by the American Physical Society.

determined by minimization of the interfacial energy, which in terms of geometric criteria is based on structural coincidences of their lattice sites. They support the view that in the case of a crystal–quasicrystal interface, lattice coincidence is not possible but the minimization of the interfacial energy is by maximizing the number of coincidences between atomic lattice sites, hence lowering the energy of the resulting interface.

3. Conclusions

The results described herein indicate that quasicrystalline materials can have and perhaps in general will always have specific orientational relationships in interfaces to crystals. These obey very similar rules to those that govern crystalline interfaces. In real space it is hard to model this, except via some large approximant to the quasicrystal, but one can come rather close to predicting what configurations will be of lower energy via a reciprocal lattice approach.

One weakness of the CRLP model is that it does not specifically analyze the structural units of the interface; rather it circumvents this issue by looking more at what is likely to be a low energy interface. One does have a similar problem in bulk materials with the CSL model which only predicts what might be low energy, but one has to go to specific atomistic calculations to verify this. At least in principle, so long as one stays within the framework of a pairwise potential the CRLP model can be expanded to include higher order terms so one can generate more accurate energies. It might also be informative to perform more detailed experimental tests. For instance, one could analyze the shape of quasicrystalline precipitates within a crystalline matrix (or vice versa) to generate the equivalent of a Wulff-construction shape and see how this compares to this or other models.

Along similar lines, one road forward to better understanding these interfaces would be via more experimental measurements focusing more on the energies rather than observations of what one has, which should provide better tests of the different models. Another interesting issue is what

(if any) role there is for the equivalent of misfit dislocations at these boundaries. For instance, it is now well established (e.g. [48]) that, like in the low angle grain boundaries case, one can have dislocation arrays at orientations near to CSL boundaries in the bulk, and misfit dislocations during epitaxial growth are also well established (e.g. [49]). It is an open question whether one can have these (we expect so, but are not aware of any reports) and whether or not one can have strain relief via the formation of (threading or non-threading) dislocations above a certain critical thickness, and an analog of pseudomorphic growth below similar to crystal–crystal epitaxy.

References

[1] Shechtman D, Blech I, Gratias D and Cahn J W 1984 *Phys. Rev. Lett.* **53** 1951
[2] Urban K, Moser N and Kronmuller H 1985 *Phys. Status Solidi* A **91** 411
[3] Zurkirch M, Bolliger B, Erbudak M and Kortan A R 1998 *Phys. Rev.* B **58** 14 113
[4] Qin Y L, Wang R H, Wang Q L, Zhang Y M and Pan C X 1995 *Phil. Mag. Lett.* **71** 83
[5] Yang X X, Wang R H and Fan X J 1996 *Phil. Mag. Lett.* **73** 121
[6] Shen Z, Kramer M J, Jenks C J, Goldman A I, Lograsso T, Delaney D, Heinzig M, Raberg W and Thiel P A 1998 *Phys. Rev.* B **58** 9961
[7] Zhang Z and Geng W 1992 *Phil. Mag. Lett.* **65** 211
[8] Zhang Z and Urban K 1989 *Scr. Metall. Mater.* **23** 1663
[9] Zhuang Y, Zhang Z and Williams D B 1993 *J. Non-Cryst. Solids* **153** 119
[10] Shimoda M, Sato T J, Tsai A P and Guo J Q 2000 *Phys. Rev.* B **62** 11288
[11] Shimoda M, Guo J Q, Sato T J and Tsai A P 2001 *Surf. Sci.* **482** 784
[12] Shimoda M, Sato T J, Tsai A P and Guo J Q 2002 *Surf. Sci.* **507** 276
[13] Sharma H R, Shimoda M and Tsai A P 2007 *Adv. Phys.* **56** 403
[14] Longchamp J-N, Burkardt S, Erbudak M and Weisskopf Y 2007 *Phys. Rev.* B **76** 094203
[15] Fournée V and Thiel P A 2005 *J. Phys. D: Appl. Phys.* **38** R83–106

[16] Li G, Zhang D, Jiang H, Lai W, Liu W and Wang Y 1997 *Appl. Phys. Lett.* **71** 897
[17] Widjaja E J and Marks L D 2003 *Phil. Mag. Lett.* **83** 47
[18] Brien V, Dauscher A, Weisbecker P and Machizaud F 2003 *Appl. Phys.* A **76** 187
[19] Willmott P R, Schlepütz C M, Herger R, Patterson B D, Hassdenteufel K and Steurer W 2005 *Phys. Rev.* B **71** 094203
[20] Saito K, Ichioka K and Sugawara S 2005 *Phil. Mag.* **85** 3629
[21] Franke K J, Gille P, Rieder K H and Theis W 2007 *Phys. Rev. Lett.* **99** 036103
[22] Widjaja E J and Marks L D 2003 *Thin Solid Films* **441** 63
[23] Rouxel D and Pigeat P 2006 *Prog. Surf. Sci.* **81** 488
[24] Wang Z G, Yang X X and Wang R H 1993 *J. Phys.: Condens. Matter* **5** 7569
[25] Shalaeva E V and Prekul A F 2006 *Phys. Met. Metallogr.* **101** 141
[26] Shen Z, Kramer M J, Jenks C J, Goldman A I, Lograsso T, Delaney D, Heinzig M, Raberg W and Thiel P A 1998 *Phys. Rev.* B **58** 9961
[27] Schwartz D, Vitek V and Sutton A P 1985 *Phil. Mag.* A **51** 499
[28] Sutton A P and Vitek V 1983 *Phil. Trans. R. Soc.* A **309** 1
[29] Sutton A P and Vitek V 1983 *Phil. Trans. R. Soc.* A **309** 55
[30] Friedel G 1926 *Lecon de Cristallographie* (Paris: Berger Levrault)
[31] Ranganathan S 1966 *Acta Crystallogr.* **21** 197
[32] Grimmer H 1974 *Acta Crystallogr.* A **30** 685
[33] Grimmer H 1974 *Acta Crystallogr.* A **30** 680
[34] Grimmer H, Bollmann W and Warrington D H 1974 *Acta Crystallogr.* A **30** 197
[35] Grimmer H 1976 *Acta Crystallogr.* A **32** 783
[36] Bolliger B, Erbudak M, Vvedensky D D, Zurkirch M and Kortan A R 1998 *Phys. Rev. Lett.* **80** 5369
[37] Flückiger T, Weisskopf Y, Erbudak M, Lüscher R and Kortan A R 2003 *Nano Lett.* **3** 1717
[38] Burkov S E 1991 *Phys. Rev. Lett.* **67** 614
[39] Abe E, Saitoh K, Takakura H, Tsai A P, Steinhardt P J and Jeong H-C 2000 *Phys. Rev. Lett.* **84** 4609
[40] Bolliger B, Dmitrienko V E, Erbudak M, Luscher R, Nissen H U and Kortan A R 2001 *Phys. Rev.* B **63** 052203
[41] Lüscher R, Erbudak M and Weisskopf Y 2004 *Surf. Sci.* **569** 163
[42] Flückiger T, Weisskopf Y, Erbudak M, Lüscher R and Kortan A R 2003 *Nano Lett.* **3** 1717
[43] Widjaja E J and Marks L D 2003 *Phys. Rev.* B **68** 134211
[44] Fletcher N H 1964 *J. Appl. Phys.* **35** 234
[45] Fletcher N H and Lodge K W 1975 *Epitaxial Growth, Part B* (New York: Academic) chapter 7, pp 529–57
[46] Giacovazzo C 1998 *Direct Phasing in Crystallography* (New York: Oxford University Press) pp 18–20
[47] Wang Z G, Yang X X and Wang R H 1993 *J. Phys.: Condens. Matter* **5** 7569
[48] Babcock S E and Balluffi R W 1987 *Phil. Mag.* A **55** 643
[49] Frank F C and van der Merwe J H 1949 *Proc. R. Soc.* A **198** 205